Frontiers in Bioscience Landmark

Front. Biosci. (Landmark Ed) **2026**; 31(4): 50109
https://doi.org/10.31083/FBL50109

Original Research

Demethylase ALKBH4 Inhibits Cell Proliferation via Induction of 5′-tsRNA^{Glu} in Non-Small Cell Lung Cancer

Chuanlin Shen[1,2,†], Haimei Cheng[1,2,†], Yiling Liu[1,2], Dandan Xu[3], Weijie Ding[1,2], Miaoyan Pu[1,2], Luyu Shi[1,2], Jiaxin Tian[4], Ying Zhang[1,2,*]

[1]Department of Biochemistry and Molecular Biology, School of Basic Medicine, Chongqing Medical University, 400016 Chongqing, China
[2]Molecular Medicine and Cancer Research Center, Chongqing Medical University, 400016 Chongqing, China
[3]Department of Laboratory Medicine, Xi'an No.1 Hospital, The First Affiliated Hospital of Northwest University, 710002 Xi'an, Shaanxi, China
[4]The First Clinical College, Chongqing Medical University, 400016 Chongqing, China
*Correspondence: zhangying@cqmu.edu.cn (Ying Zhang)
[†]These authors contributed equally.

Academic Editor: Esteban C. Gabazza
Submitted: 17 January 2026 Revised: 7 March 2026 Accepted: 17 March 2026 Published: 20 April 2026

Abstract

Background: Transfer RNA (tRNA)-derived small RNAs (tsRNAs) are an emerging class of small non-coding RNAs that play critical roles in tumor progression; however, the functions and underlying mechanisms of tsRNAs in lung cancer development remain poorly understood. Thus, this study aimed to elucidate the molecular mechanism through which alkB homolog 4, lysine demethylase (ALKBH4) influences non-small cell lung cancer (NSCLC) progression through 5′-tsRNA^{Glu}, with a particular focus on the role of tsRNA in translational regulation and malignant phenotype formation. **Methods**: Cell proliferation and cell cycle progression were assessed using Cell Counting Kit-8 (CCK-8), colony formation, and flow cytometry assays. Global translation efficiency was evaluated using nascent protein synthesis assays and polysome profiling. Northern blotting was used to confirm 5′-tsRNA^{Glu} expression post-transfection, and downstream targets of 5′-tsRNA^{Glu} were screened using a dual-luciferase reporter system. RNA pull-down and RNA immunoprecipitation (RIP) assays were employed to identify proteins that interacted with 5′-tsRNA^{Glu}. Data were analyzed using Student's *t*-test or one-way analysis of variance (ANOVA). **Results**: The demethylase ALKBH4 promoted the biogenesis of 5′-tsRNA^{Glu} in NSCLC cells. Overexpression of ALKBH4 or 5′-tsRNA^{Glu} inhibited cell proliferation, induced cell cycle arrest, and reduced global translational efficiency, whereas knockdown of 5′-tsRNA^{Glu} attenuated the tumor-suppressive effects of ALKBH4. Mechanistically, 5′-tsRNA^{Glu} did not function in a miRNA-like manner but instead interacted with ribosomal protein L17 (RPL17). Furthermore, 5′-tsRNA^{Glu} was predominantly localized in the cytoplasm, and 5′-tsRNA^{Glu} overexpression significantly increased the associated distribution in the 60S ribosomal subunit while diminishing the associated presence in the 80S monosome. Predictive modeling indicated that 5′-tsRNA^{Glu} binds to the region of RPL17 spanning residues 137–142, the RPL17–rRNA interaction interface, suggesting that binding of 5′-tsRNA^{Glu} to RPL17 interferes with RPL17–rRNA interaction, thereby disrupting the 80S ribosome assembly and global translational efficiency. **Conclusions**: ALKBH4 suppresses malignant phenotypes in NSCLC cells via 5′-tsRNA^{Glu}, likely through an interaction between 5′-tsRNA^{Glu} and RPL17.

Keywords: non-small cell lung cancer; non-coding RNA; demethylase; translation

1. Introduction

Lung cancer is one of the most prevalent malignant tumors worldwide and ranks first in both incidence and mortality among all malignancies in China, showing no significant decline over the past decade [1]. Non-small cell lung cancer (NSCLC) accounts for approximately 85% of all lung cancer cases, with lung adenocarcinoma (LUAD) and lung squamous cell carcinoma (LSCC) being the most common histological subtypes. The five-year survival rate of patients with NSCLC is approximately 15.9%, largely owing to challenges related to early detection and effective precision treatment regimens [2]. Therefore, elucidating the molecular mechanisms of NSCLC-related genes holds significant promise for the development of novel strategies for early diagnosis and targeted therapy.

tRNA-derived small RNAs (tsRNAs) constitute an emerging category of non-coding RNAs (ncRNAs) that are generated through the specific cleavage of mature or precursor tRNAs by ribonucleases. Fragments originating from the 5′- and 3′-ends of mature tRNAs are designated as 5′-tsRNAs and 3′-tsRNAs, respectively [3–6]. As functional tRNA derivatives [7], tsRNAs have been implicated in a diverse range of biological processes, including stress responses, translational regulation, ribosome biogenesis, and transgenerational epigenetic inheritance [8–18]. For instance, under stress conditions, such as hypoxia, amino acid deprivation, oxidative stress, or ultraviolet (UV) irradiation, angiogenin (ANG) specifically cleaves tRNAs within the anticodon loop to produce tsRNAs, also known as tRNA-derived stress-induced RNAs (tiRNAs) [8,19,20]. tsRNAs

are known to regulate translation via multiple mechanisms, such as inhibiting the initiation of translation by their unique RNA G-quadruplex (RG4) structures [10–13,21], suppressing the initiation of translation by specific tsRNA modifications [14,15], repressing the translation of target mRNA in a miRNA-like manner [16], binding to ribosomes to either halt or promote translation [17], and altering mRNA secondary structures to enhance translational efficiency [18].

tsRNAs represent a promising frontier for deciphering the complexity of malignancies. Through their distinct sequence characteristics, modification patterns, and structural configurations, tsRNAs exert context-dependent functions as either tumor suppressors or promoters [18,20,22–31]. To date, the precise function of tsRNAs in lung cancer remains largely unexplored. Specifically, tsRNA-46, tsRNA-47, and tsRNA-53 are shown to be downregulated in NSCLC samples and reduce the clonogenic capacity of NSCLC cells [23,32]. Another study identified that a tsRNA (denoted as CAT1) is upregulated across multiple cancer types; CAT1 competitively binds to the RBPMS protein with NOTCH2 mRNA, thereby inhibiting the CCR4-NOT-mediated deadenylation of NOTCH2 mRNA, increasing its stability, and ultimately facilitating the proliferation and metastasis of NSCLC cells [33]. Collectively, these findings highlight the pivotal regulatory functions of tsRNAs in the progression of NSCLC. Consequently, a systematic investigation of tsRNAs will advance our understanding of the molecular mechanisms underlying NSCLC and support the development of innovative diagnostic and therapeutic approaches. In a previous study, we developed PANDORA-seq, a novel sequencing platform for small non-coding RNA, and discovered a 36-nt 5′-tsRNA derived from specific cleavage within the anticodon loop of $tRNA^{Glu(CTC)}$, termed 5′-$tsRNA^{Glu}$. In addition, we found that 5′-$tsRNA^{Glu}$ positively regulated embryonic stem cell differentiation and attenuated translational efficiency [34]. From a comparative medical standpoint, it is likely that 5′-$tsRNA^{Glu}$ may act as a potential tumor suppressor, especially given that tumors often exhibit features of dedifferentiation and enhanced translation.

tRNAs are more extensively decorated with chemical modifications than other RNA species, with methylation being the most abundant modification. The dynamic regulation of tRNA methylation is orchestrated by tRNA methyltransferases and demethylases [35]. Demethylation compromises the structural stability of tRNAs, rendering them more susceptible to cleavage by ribonucleases, leading to the production of tsRNAs [7,36]. The ALKBH (alpha-ketoglutarate-dependent dioxygenase alkB homolog) family is a class of Fe^{2+}- and α-ketoglutarate-dependent dioxygenases, comprising nine members, namely ALKBH1 to ALKBH8 and FTO, that mediate a myriad of biological processes. Among their key functions is tRNA demethylation [37–39]. Our analysis of The Cancer Genome Atlas (TCGA) data indicated that ALKBH4 was differentially expressed in both LUAD and LSCC, and its elevated expression was correlated with favorable prognosis. Based on these findings, we sought to determine whether ALKBH4 serves as a tRNA demethylase responsible for modulating the biogenesis of 5′-$tsRNA^{Glu}$.

In this study, we demonstrated that ALKBH4 promoted the generation of 5′-$tsRNA^{Glu}$ in NSCLC cells and that both ALKBH4 and 5′-$tsRNA^{Glu}$ suppressed their proliferative capabilities and global translational efficiency. These mechanisms involved the interaction between 5′-$tsRNA^{Glu}$ and ribosomal proteins.

2. Materials and Methods

2.1 Cell Lines

Human NSCLC cell lines H1299 and A549 were obtained from the Cell Bank of the Type Culture Collection of the Chinese Academy of Sciences (Shanghai, China). All the cell lines were validated by STR profiling and tested negative for mycoplasma.

2.2 Construction of the ALKBH4 Expression Plasmid

pCDH-Puro-3Flag was utilized as the vector to construct the ALKBH4 expression plasmid. Briefly, the ALKBH4 coding sequence was amplified using primers designed with homologous arms flanking insertion sites. Concurrently, the pCDH-Puro-3Flag vector was linearized through PCR amplification to eliminate the original coding sequence. Both PCR products were then subjected to *in vitro* recombination using the NovoRec® One-Step PCR Cloning Kit (Novoprotein, Suzhou, China) in a molar ratio-based reaction system. The ligation product was transformed into TransStbl3 competent cells and plated onto LB agar plates supplemented with ampicillin for colony growth. Positive clones were screened utilizing colony PCR. The ALKBH4 expression plasmid was subsequently verified by sequencing (Sangon Biotech, Shanghai, China).

2.3 Cell Treatment and Transfection

For H_2O_2 treatment, H_2O_2 solution (Sigma-Aldrich, MO, USA) was diluted in complete medium and cells were treated with H_2O_2 solution at designated concentrations for 24 h. The cells were then collected and analyzed. For plasmid transfection, cells were transiently transfected with 2 µg of ALKBH4 plasmid or pCDH-Puro-3Flag plasmid using Neofect DNA Transfection Reagent (Neofect, Beijing, China) according to the manufacturer's instructions. For RNA transfection, cells were transiently transfected with mimics, antisense oligonucleotides (ASO), or corresponding controls at a final concentration of 50 nM using Lipofectamine™ RNAiMAX reagent (Thermo Fisher Scientific, MA, USA) according to the manufacturer's instructions. Cells were collected and analyzed 24 h after transfection. 5′-$tsRNA^{Glu}$ mimics and 5′-$tsRNA^{Glu}$-targeting ASO were chemically synthesized (Sangon Biotech, Shanghai, China). The oligonucleotide sequences are listed in **Supplementary Table 1**.

2.4 Cell Proliferation and Colony Formation Assays

For cell proliferation assays, cells were seeded in 96-well plates at a density of 1000 cells per well. Cell proliferation was subsequently measured using a Cell Counting Kit-8 (Bimake, TX, USA) according to the manufacturer's instructions. The absorbance of each well was measured at 450 nm at each time point. For colony formation assays, cells were seeded in 6-well plates at a density of 1000 cells per well. After incubation at 37 °C for approximately 14 days, cells were washed three times with PBS, fixed with 4% paraformaldehyde for 30 min, and stained with 0.2% crystal violet solution for 30 min. After washing three times with PBS, each well was photographed, and the number of colonies was counted. Three independent experiments were performed, each in triplicate.

2.5 Cell Cycle Analysis

Cells were harvested and washed twice in PBS, suspended in 700 µL of 75% ethanol, mixed with 300 µL of PBS, and refrigerated at –20 °C overnight. Following centrifugation and washing twice with PBS, cells were resuspended, stained with propidium iodide (PI)/RNase Stain Binding Buffer, and placed at 4 °C for 30 min. DNA content was then measured using a FACSCalibur flow cytometer (BD Biosciences, CA, USA). Three independent experiments were performed, each in triplicate.

2.6 OPP Protein Synthesis Assays

Experiments were performed using the Click-iT Plus OPP Protein Synthesis Assay Kit (Invitrogen, CA, USA). Briefly, cells in 6-well plates were incubated with 1 mL of medium containing 10 µM Click-iT Plus OPP working solution for 15 min. After centrifugation and washing with PBS, cells were fixed in 3.7% paraformaldehyde for 15 min, permeabilized in 0.5% Triton X-100 for 15 min, and then incubated in the dark with 100 µL of Click-iT Plus OPP reaction cocktail for 30 min. Subsequently, the cells were washed with the Click-iT reaction rinse buffer and stained with 4′,6-diamidino-2-phenylindole (DAPI). Samples were then analyzed using a FACSCanto II flow cytometer (BD Biosciences, CA, USA). Three independent experiments were performed, each in triplicate.

2.7 Polysome Profiling

Cells were treated with 100 µg/mL cycloheximide (CHX) for 5 min, lysed with lysis buffer (20 mM Tris-HCl, pH 7.5, 2.5 mM $MgCl_2$, 150 mM NaCl, 100 µg/mL of CHX, 1 mM DTT, 100 U/mL of RNasein, 0.5% Triton X-100) on ice; subsequently, the cells were centrifuged and the supernatant was collected. The supernatant was layered on top of a 5–45% (w/v) sucrose gradient and centrifuged at 32,000 rpm at 4 °C for 1.5 h. Subsequently, the sample was fractionated using a Gradient Fractionator (Biocomp, Quebec, Canada) while continuously monitoring the absorbance at 260 nm. Fractions were categorized and used to isolate total RNA for subsequent RNA analysis. Three independent experiments were performed, each in triplicate.

2.8 Dual-Luciferase Reporter Assays

The 5′-tsRNA^{Glu} target sequence (reverse complement to the 5′-tsRNA^{Glu} sequence) was subcloned into the pmirGLO vector (Tsingke, Beijing, China). Subsequently, the cells were co-transfected with the reporter plasmid and 5′-tsRNA^{Glu} mimics or NC mimics using Lipofectamin^{TM} 3000 (Invitrogen, CA, USA). 24 h post-transfection, firefly and renilla luciferase activities were quantified using the Dual-Luciferase Reporter Assay System (Beyotime, Shanghai, China) following the manufacturer's protocol. Three independent experiments were performed, each in triplicate.

2.9 Nuclear and Cytoplasmic RNA Fractionation

Cells were washed with PBS and harvested by centrifugation. Nuclear and cytoplasmic extracts were then prepared using a Nuclear and Cytoplasmic Protein Extraction Kit (Beyotime, Shanghai, China) following the manufacturer's instructions. Briefly, cell pellets were resuspended in Reagent A, vortexed, and then incubated on ice. Following the addition of Reagent B and vortexing, the mixture was incubated on ice and centrifuged to separate the supernatant (containing cytoplasmic proteins) from the pellet (containing nuclear proteins). Cytoplasmic and nuclear RNAs were extracted from these fractions by adding TRIzol^{TM} reagent (Invitrogen, CA, USA). Three independent experiments were performed, each in triplicate.

2.10 RNA Pull-Down Assays

Biotin-labeled 5′-tsRNA^{Glu} and its antisense probe were synthesized by Sangon Biotechnology (Shanghai, China). RNA pull-down assays were then conducted using the Pierce^{TM} Magnetic RNA-Protein Pull-Down Kit (Thermo Fisher Scientific, MA, USA) according to the manufacturer's instructions. Briefly, 100 pmol of biotin-labeled 5′-tsRNA^{Glu} or its antisense probe was added to 50 µL of streptavidin-coated magnetic beads and incubated for 30 min under constant agitation. The Master Mix containing pre-prepared cell lysates was then added to the RNA-bound beads and incubated at 4 °C for 60 min. Subsequently, the beads were washed three times with wash buffer, resuspended in loading buffer, followed by denaturation at 100 °C for 10 min. Eluted proteins were then separated by SDS-PAGE and visualized using Coomassie Blue staining. Protein bands within the molecular weight range of 20–150 kDa were excised and subjected to protein identification using LC-MS/MS on a Q-Exactive HF X tandem mass spectrometer (Thermo Fisher Scientific, CA, USA) at BGI (Shenzhen, China). The sequences of all RNA pull-down probes are provided in **Supplementary Table 1**. Three independent experiments of RNA pull-down assay were performed, each in triplicate.

2.11 RNA Immunoprecipitation (RIP) Assays

RIP assays were conducted using an Immunoprecipitation Kit with Protein A+G Magnetic Beads (Beyotime, Shanghai, China), according to the manufacturer's protocol. Briefly, cells were lysed in RIP lysis buffer containing protease inhibitors and RNase inhibitors. The lysate was centrifuged, and then the supernatant was collected and incubated with 0.5 µg of RPL17 antibody (14121-1-AP, Proteintech, IL, USA) or IgG antibody (A7016, Beyotime, Shanghai, China) under rotation at 4 °C for 24 h. Subsequently, 10 µL of Protein A+G magnetic beads were added and incubated with rotation at 4 °C for 16 h. RNA bound to the immunoprecipitated complexes was extracted using TRIzol™ reagent (Invitrogen, CA, USA) and subjected to quantitative RT-PCR analysis. Three independent experiments were performed, each in triplicate.

2.12 RNA Isolation and Quantitative RT-PCR

Total RNA was isolated from cell lines using TRIzol™ reagent (Invitrogen, CA, USA), according to the manufacturer's protocol. To detect small RNAs, cDNA was reverse-transcribed from 500 ng of total RNA using the PrimeScript™ II 1st Strand cDNA Synthesis Kit (Takara, Tokyo, Japan). For mRNA detection, cDNA was synthesized from 500 ng of total RNA using a PrimeScript™ RT Master Mix Kit (Takara, Tokyo, Japan). Quantitative real-time PCR was performed using 2×SYBR Green qPCR Master Mix (Bimake, TX, USA). U6 and GAPDH served as internal controls to normalize the expression levels of 5′-tsRNA^{Glu} and mRNAs, respectively. Relative quantification of targets was calculated using the $2^{-\Delta\Delta Ct}$ method. All primer sequences are provided in **Supplementary Table 1**.

2.13 Northern Blotting

Total RNAs were resolved on a 10% urea-PAGE gel and stained with SYBR Gold (Thermo Fisher Scientific, MA, USA), followed by immediate imaging. The separated RNAs were then transferred onto positively charged nylon membranes (Roche, Basel, Switzerland) and ultraviolet-crosslinked at an energy of 0.12 J. Subsequently, membranes were pre-hybridized with DIG Easy Hyb solution (Roche, Basel, Switzerland) for 1 h at 42 °C. After pre-hybridization, membranes were hybridized overnight at 42 °C with a DIG-labeled 5′-tsRNA^{Glu} probe (Sangon Biotech, Shanghai, China). The probe sequences are listed in **Supplementary Table 1**. Subsequently, membranes were washed, blocked, and incubated with an anti-DIG-AP antibody (11093274910, 1:10,000, Roche, Basel, Switzerland) for 30 min. Signal detection was performed using the chemiluminescent substrate CSPD (Roche, Basel, Switzerland), and visualization was performed using a ChemiDoc™ MP Imaging System (Bio-Rad, CA, USA).

2.14 Western Blotting

Western blot analysis was performed according to a previously established protocol [40]. The following primary antibodies were used: rabbit monoclonal anti-ALKBH4 (ab195379, 1:1000, Abcam, Cambridge, UK), rabbit polyclonal anti-Cyclin D1 (AF0126, 1:1000, Beyotime, Shanghai, China), rabbit polyclonal anti-RPL17 (14121-1-AP, 1:1000, Proteintech, IL, USA), rabbit polyclonal anti-Cyclin B1 (55004-1-AP, 1:1000, Proteintech, IL, USA), rabbit polyclonal anti-Phospho-Histone-H3 (9701, 1:1000, Cell Signaling Technology, MA, USA), rabbit monoclonal anti-Histone-H3 (4499T, 1:1000, Cell Signaling Technology, MA, USA), rabbit polyclonal anti-GAPDH (AB-P-R001, 1:1000, Goodhere Biotech, Hangzhou, China), and rabbit monoclonal anti-β-actin (T40104, 1:1000, Abmart, Shanghai, China).

2.15 RNA Sequencing

H1299 cells were transiently transfected for 24 h with the pCDH plasmid, ALKBH4 expression plasmid, NC mimics, and 5′-tsRNA^{Glu} mimics, as indicated. Total RNA was extracted using TRIzol™ reagent (Invitrogen, CA, USA). Following quantitative analysis and quality inspection, the RNA samples were subjected to sequencing by BGI (Shenzhen, China). Libraries were constructed using the Optimal Dual-mode mRNA Library Prep Kit (BGI, Shenzhen, China), and sequenced on a BGIseq500 platform (BGI, Shenzhen, China). Raw sequencing data were normalized for subsequent analysis. RNA-seq data are shown in **Supplementary Table 2**. Differentially expressed genes were identified using a threshold of $|\log2 \text{ (fold change)}| \geq 1$ and adjusted p-value < 0.05.

2.16 Bioinformatic Analysis

RNA sequencing data for both LUAD and LSCC tissues were retrieved from the TCGA database [41]. Co-correlation patterns between ALKBH4 and other genes were evaluated using Pearson's correlation analysis [42]. Gene Set Enrichment Analysis (GSEA) was performed with the GSEA portal (https://www.gsea-msigdb.org/gsea/index.jsp) with the "C5.go.bp.v7.5.symbols.gmt" gene set collection. The selection criteria were as follows: nominal p-value < 0.05, false discovery rate (FDR) <0.25, and gene set size >100. Target gene prediction for 5′-tsRNA^{Glu} was conducted using the TargetRank database (https://www.targetscan.org/vert_80/) [43]. The interaction probabilities between 5′-tsRNA^{Glu} and candidate proteins were forecast using RPIseq (http://pridb.gdcb.iastate.edu/RPISeq/). Molecular docking simulations of 5′-tsRNA^{Glu} and RPL17 were conducted using the HDOCK server (http://hdock.phys.hust.edu.cn/).

2.17 Statistical Analysis

Statistical analyses were performed using SPSS software (version 22.0, SPSS Inc., IL, USA). Comparisons be-

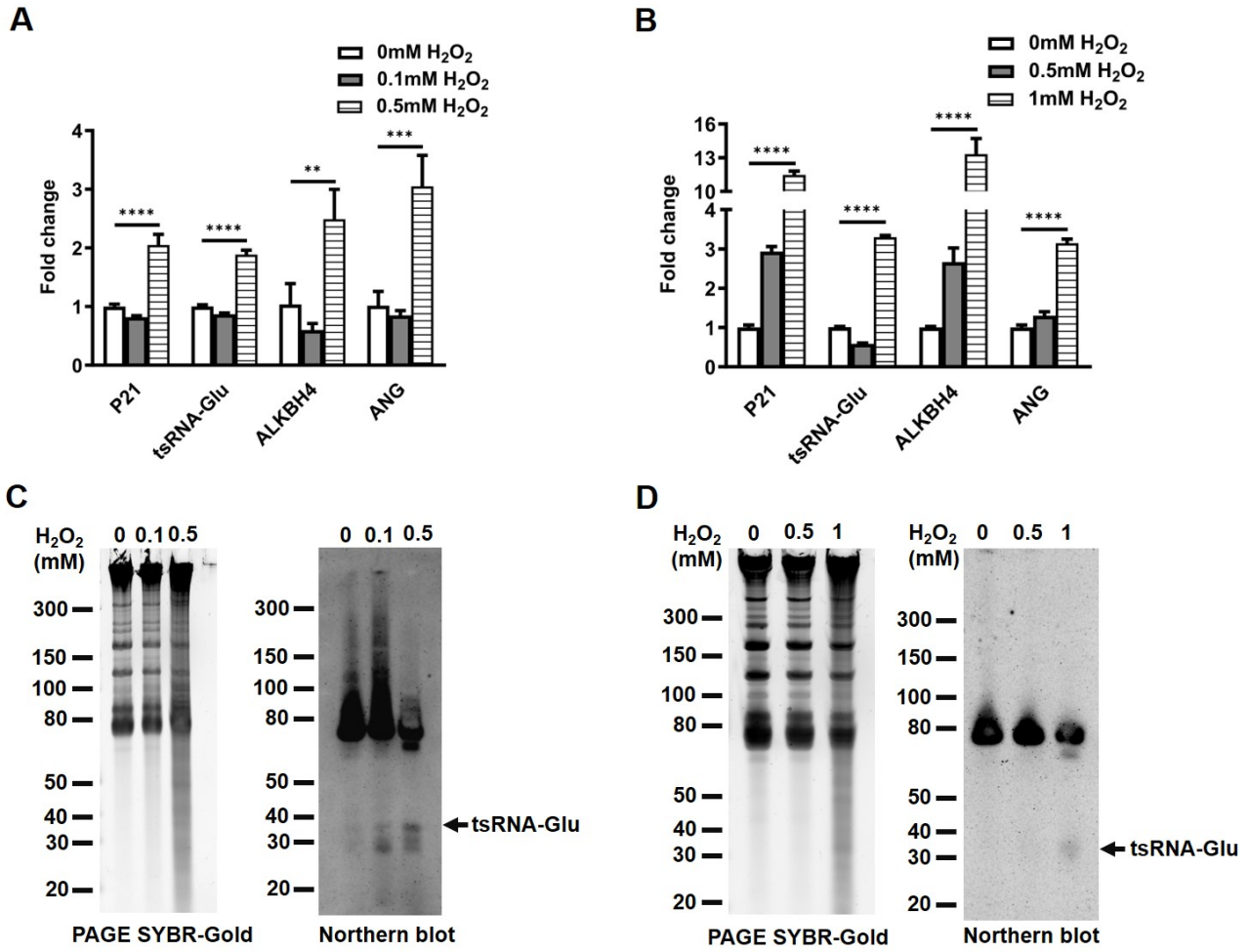

Fig. 1. The levels of 5′-tsRNA^{Glu}, ALKBH4 and ANG in NSCLC cells treated with H_2O_2. (A,B) The levels of 5′-tsRNA^{Glu}, ALKBH4 and ANG in H1299 cells (A) and A549 cells (B) treated with H_2O_2 were measured using quantitative RT-PCR, with U6 and GAPDH as the loading controls, respectively. (C,D) The 5′-tsRNA^{Glu} levels in H1299 cells (C) and A549 cells (D) treated with H_2O_2 were measured using Northern blot. The overall band intensity in PAGE served as the loading control. Data are shown as the mean ± SD (one-way ANOVA, ** $p < 0.01$, *** $p < 0.001$ and **** $p < 0.0001$). Note: tsRNA-Glu is the abbreviation of 5′-tsRNA^{Glu}.

tween two groups were assessed using unpaired two-tailed Student's *t*-test, while comparisons among multiple groups were performed using one-way ANOVA. *p*-value < 0.05 was considered statistically significant.

3. Results

3.1 Oxidative Stress Induced the Generation of 5′-tsRNA^{Glu} and ALKBH4 in NSCLC Cells

5′-tsRNA^{Glu} (36-nt in length), is produced from the specific cleavage of the anticodon loop of tRNA$^{Glu(CTC)}$. The type of 5′-tsRNA is also addressed by another name, *i.e.*, tiRNA, in response to stress conditions. To test if 5′-tsRNA^{Glu} was induced by oxidative stress, we compared the levels of 5′-tsRNA^{Glu} in NSCLC cells responding to H_2O_2 treatment. H1299 cells subjected to H_2O_2 treatment exhibited a significant increase in the levels of 5′-tsRNA^{Glu}, ALKBH4, and ANG (Fig. 1A,C). Similarly, their expression levels were remarkably upregulated in A549 cells following the H_2O_2 treatment (Fig. 1B,D). Oxidative stress increased the levels of 5′-tsRNA^{Glu} in NSCLC cells. Under the same conditions, the expression of ALKBH4 and ANG was also elevated, suggesting that these factors are responsive to oxidative stress.

3.2 ALKBH4 Induced the Biogenesis of 5′-tsRNA^{Glu} in NSCLC Cells

RNA sequencing data for LUAD and LSCC were downloaded from the TCGA database and then used for gene expression correlation analysis, further creating a set of genes that were highly correlated with ALKBH4 expression. GSEA revealed that the gene set correlated with ALKBH4 was remarkably enriched in 'tRNA processing' and 'RNA methylation' (**Supplementary Fig. 1**), thus indicating that ALKBH4 might mediate the dynamic methylation of tRNAs.

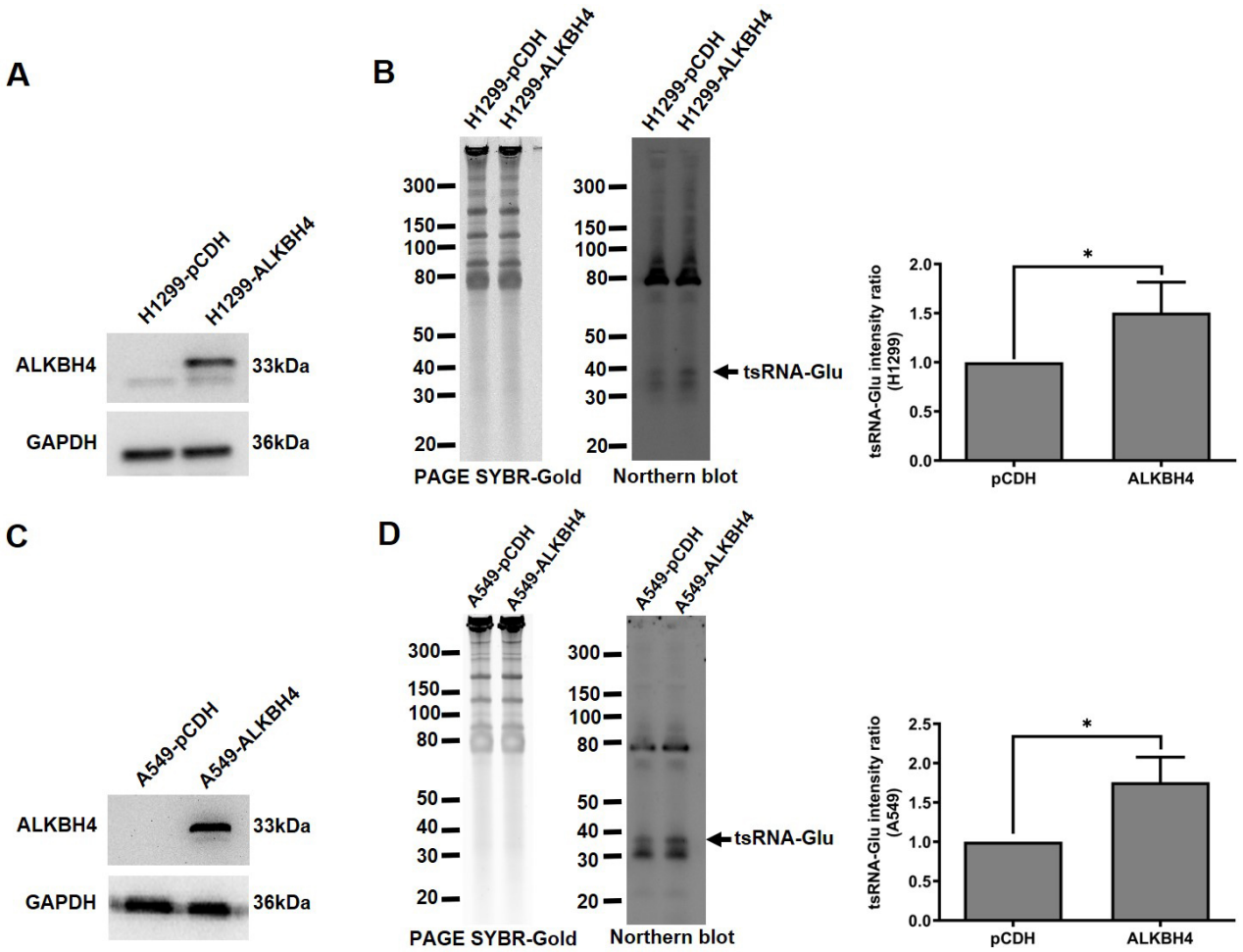

Fig. 2. The 5′-tsRNA^{Glu} levels in NSCLC cells overexpressing ALKBH4. The ALKBH4 levels in H1299 cells (A) and A549 cells (C) transiently transfected with the ALKBH4 plasmid were determined using Western blot. GAPDH served as the loading control. The 5′-tsRNA^{Glu} levels in H1299 cells (B) and A549 cells (D) transiently transfected with the ALKBH4 plasmid were determined using Northern blot. The overall band intensity in PAGE served as the loading control. The right panel shows the densitometric quantification of 5′-tsRNA^{Glu} levels, presented as fold change relative to the control group. Data are shown as the mean ± SD from three independent experiments (two-sided independent Student's *t*-test, * $p < 0.05$). Note: tsRNA-Glu is the abbreviation of 5′-tsRNA^{Glu}.

Furthermore, NSCLC cells were transfected with the ALKBH4 plasmid (Fig. 2A,C). Both H1299 cells and A549 cells with ectopic expression of ALKBH4 showed a significant increase in 5′-tsRNA^{Glu} levels (Fig. 2B,D). These results suggest that ALKBH4 may induce the biogenesis of 5′-tsRNA^{Glu} in NSCLC cells, potentially through its tRNA demethylase activity. However, to determine whether ALKBH4 directly induces the biogenesis of 5′-tsRNA^{Glu}, further studies will need to evaluate 5′-tsRNA^{Glu} levels in ALKBH4 knockout cells.

3.3 ALKBH4 and 5′-tsRNA^{Glu} Inhibited the Proliferation of NSCLC Cells

Next, we ivestigated the effects of ALKBH4 and 5′-tsRNA^{Glu} on the proliferative ability of NSCLC cells. H1299 cells exhibiting ectopic ALKBH4 expression showed a remarkable reduction in cell proliferation, colony formation, and cell cycle arrest at the S-phase (Fig. 3). Likewise, H1299 cells transiently transfected with 5′-tsRNA^{Glu} mimics revealed decreased capabilities for cell proliferation, colony formation, and cell cycle arrest at the G2/M phase (Fig. 4A–E). Conversely, the knockdown of 5′-tsRNA^{Glu} using its specific ASO significantly promoted the cell proliferation and colony formation of H1299 cells (**Supplementary Fig. 2**). Furthermore, the reduction in cell proliferation due to ALKBH4 overexpression was rescued by the knockdown of 5′-tsRNA^{Glu} (Fig. 4F). Collectively, these results suggest that ALKBH4 inhibited NSCLC cell proliferation probably via the induction of 5′-tsRNA^{Glu}.

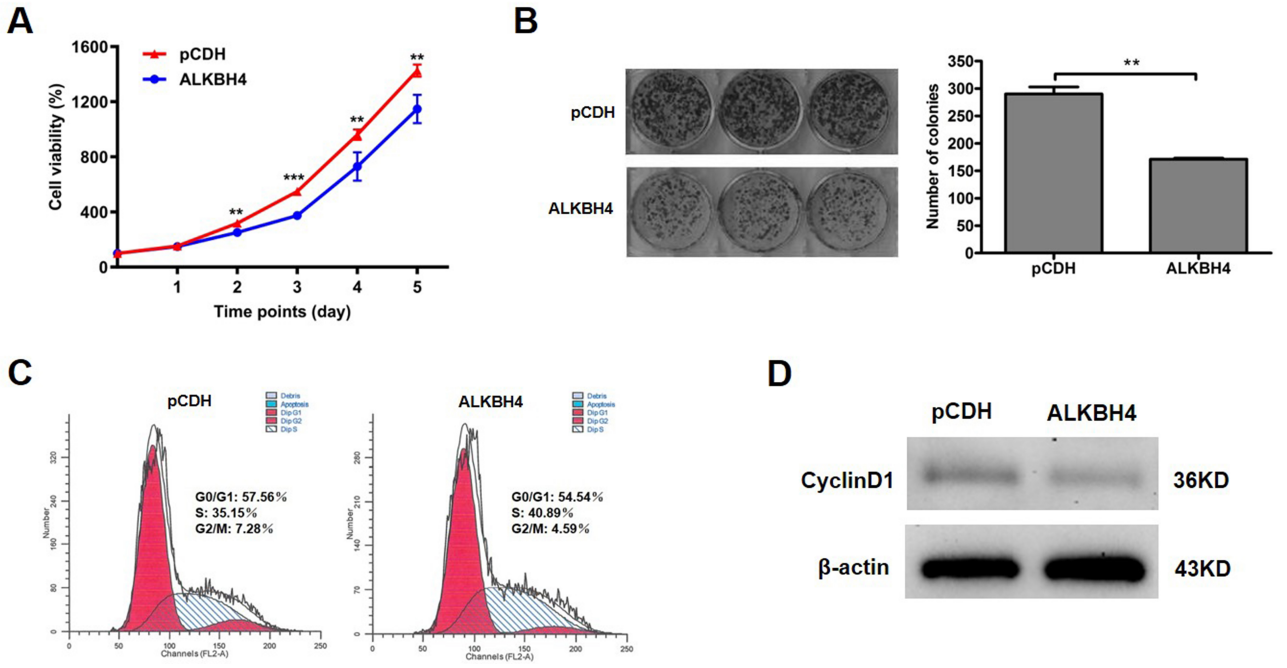

Fig. 3. The effects of ALKBH4 on cell proliferation and cell cycle of H1299 cells. (A) Proliferation curves of H1299 cells transiently transfected with the ALKBH4 plasmid or the pCDH vector were monitored every 24 h, over 5 days. Three independent experiments were performed in triplicate. Data are shown as the mean ± SD (two-sided independent Student's *t*-test, ** $p < 0.01$ and *** $p < 0.001$). (B) Representative images of the colony formation of H1299 cells transiently transfected with the ALKBH4 plasmid or the pCDH vector were photographed (left). Their corresponding colony numbers were enumerated (right). Three independent experiments were performed in triplicate. Data are shown as the mean ± SD (two-sided independent Student's *t*-test, ** $p < 0.01$). (C) The cell cycle of H1299 cells transiently transfected with the ALKBH4 plasmid or the pCDH vector was detected using flow cytometry. (D) The CyclinD1 level in H1299 cells transiently transfected with the ALKBH4 plasmid was determined using Western blot. β-actin served as the loading control.

3.4 ALKBH4 and 5′-tsRNA^{Glu} Repressed Global Translational Efficiency

We further evaluated the effects of ALKBH4 and 5′-tsRNA^{Glu} on protein synthesis in NSCLC cells. OPP protein synthesis assays showed that the overexpression of ALKBH4 decreased nascent protein synthesis in H1299 cells (Fig. 5A). Furthermore, the overexpression of ALKBH4 reduced 80S monosome and polysome contents in polysome profiling (Fig. 5B). Consistently, the overexpression of 5′-tsRNA^{Glu} receded nascent protein synthesis as well as 80S monosome and polysome contents in H1299 cells (Fig. 5C,D). Overall, these results indicate that both ALKBH4 and 5′-tsRNA^{Glu} contributed to the downregulation of global translation efficiency in NSCLC cells.

3.5 5′-tsRNA^{Glu} Functioned Differently From miRNAs

Previous studies have established that tsRNAs can inhibit the translation of mRNAs via binding complementarily with the 3′UTR of these mRNAs, in a miRNA-like manner [22,24,28,44–47]. Based on this, we proceeded to screen the target mRNAs of 5′-tsRNA^{Glu}. The mRNA expression profiles of NSCLC cells transiently transfected with the ALKBH4 plasmid (termed the ALKBH4 profile) and those with 5′-tsRNA^{Glu} mimics (termed the tsRNA-Glu profile) were detected using RNA sequencing. GSEA revealed that the biological process categories enriched in the ALKBH4 profile were translational termination, ribosome biogenesis, ncRNA processing, *etc.* (**Supplementary Fig. 3A**). The biological process categories enriched in the tsRNA-Glu profile were the regulation of response to extracellular stimulus, the negative regulation of epithelial cell proliferation, and drug catabolic process, among others (**Supplementary Fig. 3B**). It displayed 11 differentially expressed genes with the same trend in the ALKBH4 profile and the tsRNA-Glu profile (**Supplementary Table 3**). Of these, three genes that strongly associated with tumor progression, *i.e.*, XAF1, EIF2S3B and REC8, were selected for further validation using quantitative RT-PCR. It showed that EIF2S3B and REC8 were significantly upregulated in both profiles, consistent with the RNA sequencing results, whereas XAF1 expression displayed the contrary tendency in both profiles (**Supplementary Fig. 4A,B**). Subsequently, we analyzed the expression patterns of XAF1 and REC8 in NSCLC tumor tissues compared to normal lung tissues, based on the TCGA and GTEx database (EIF2S3B data were unavailable). The expression levels of XAF1 and REC8 in LUAD and LSCC tissues were markedly lower than those in normal lung tissues (**Supplementary Fig.**

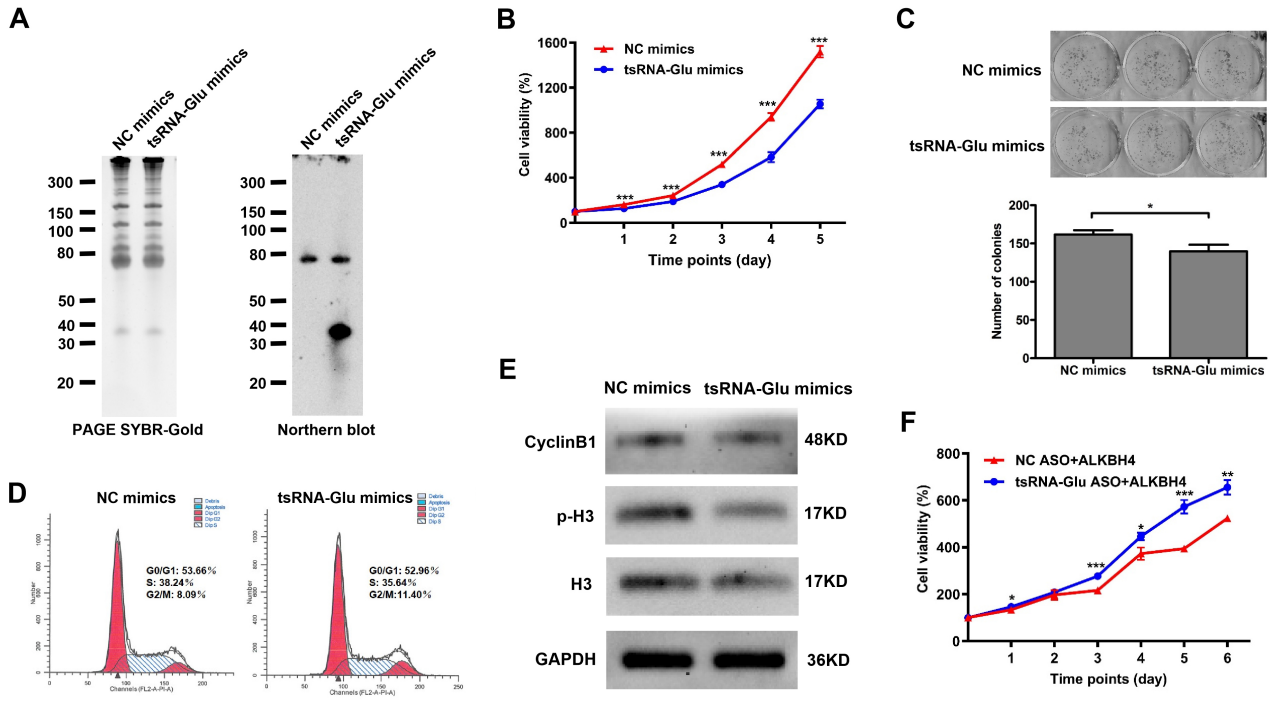

Fig. 4. The effects of 5′-tsRNA^{Glu} on cell proliferation and cell cycle of H1299 cells. (A) The 5′-tsRNA^{Glu} level in H1299 cells transiently transfected with 5′-tsRNA^{Glu} mimics was determined using Northern blot. The overall band intensity in PAGE served as the loading control. (B) Proliferation curves of H1299 cells transiently transfected with 5′-tsRNA^{Glu} mimics or NC mimics were monitored every 24 h, over 5 days. Three independent experiments were performed in triplicate. Data are shown as the mean ± SD (two-sided independent Student's *t*-test, *** $p < 0.001$). (C) Representative images of the colony formation of H1299 cells transiently transfected with 5′-tsRNA^{Glu} mimics or NC mimics were photographed (top). Their corresponding colony numbers were enumerated (bottom). Three independent experiments were performed in triplicate. Data are shown as the mean ± SD (two-sided independent Student's *t*-test, * $p < 0.05$). (D) The cell cycle of H1299 cells transiently transfected with 5′-tsRNA^{Glu} mimics or NC mimics was detected using flow cytometry. (E) The levels of CyclinB1, phospho-H3 and H3 in H1299 cells transiently transfected with 5′-tsRNA^{Glu} mimics were determined using Western blot. GAPDH served as the loading control. (F) H1299 cells with ectopic expression of ALKBH4 were transiently transfected with the 5′-tsRNA^{Glu} ASO or NC ASO, and proliferation curves were monitored every 24 h, over 6 days. Three independent experiments were performed in triplicate. Data are shown as the mean ± SD (two-sided independent Student's *t*-test, * $p < 0.05$, ** $p < 0.01$, and *** $p < 0.001$). Note: tsRNA-Glu is the abbreviation of 5′-tsRNA^{Glu}.

4C,D). These findings imply that REC8 mRNA may represent a downstream target of 5′-tsRNA^{Glu}. Nevertheless, sequence alignment analysis failed to identify complementary pairing between 5′-tsRNA^{Glu} and all regions of the REC8 mRNA, thus indicating that REC8 mRNA is probably not the direct target of 5′-tsRNA^{Glu}.

Moreover, utilizing the TargetRank database, we predicted PPM1F, MECP2 and C14orf172 as the targets of 5′-tsRNA^{Glu}. However, subsequent validation disproved these predictions (**Supplementary Fig. 5A,B**). To directly test the gene-silencing activity of 5′-tsRNA^{Glu}, we next constructed a dual-luciferase reporter that has the complementary sequence of 5′-tsRNA^{Glu} at the 3′UTR of the Renilla luciferase gene (**Supplementary Fig. 5C,D**). The dual-luciferase reporter gene assay revealed that 5′-tsRNA^{Glu} had no effect on the relative luciferase activity of the reporter gene containing the complementary sequence of 5′-tsRNA^{Glu} (**Supplementary Fig. 5E–H**). Taking the inhibitory effects of 5′-tsRNA^{Glu} on global translation efficiency into consideration, we propose that 5′-tsRNA^{Glu} interacts with specific proteins rather than specific mRNAs, to suppress the global translation efficiency of NSCLC cells and thus their malignant phenotypes.

3.6 5′-tsRNA^{Glu} Interacted With RPL17

To verify the hypothesis that 5′-tsRNA^{Glu} could suppress global translational efficiency via binding target proteins, we next employed RNA pull-down coupled with mass spectrometry to identify proteins that interacted with 5′-tsRNA^{Glu} (Fig. 6A). Based on the results of two replicates, we identified seven overlapping proteins, including MYEF2, RPS5, RPL17, DEK, NUDT21, SRSF10, and SRSF5 (Fig. 6B). Subsequently, the interaction probabilities between 5′-tsRNA^{Glu} and the candidate proteins were predicted using the RPIseq database; RPL17 exhibited the highest interaction probability among these candidate pro-

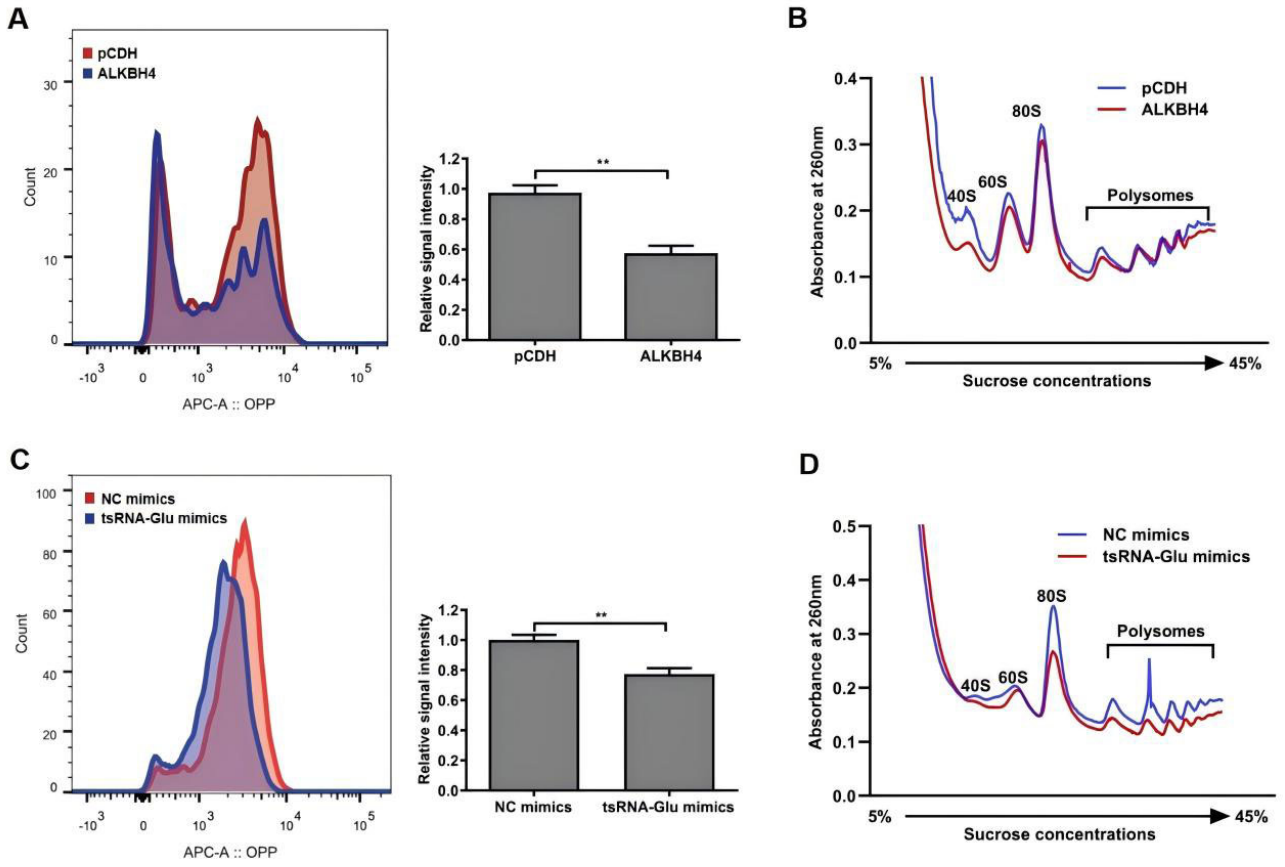

Fig. 5. The effects of ALKBH4 and 5′-tsRNA^{Glu} on the global translational efficiency of H1299 cells. (A) The nascent protein synthesis of H1299 cells transiently transfected with the ALKBH4 plasmid or the pCDH vector was determined using OPP protein synthesis assay. Their relative fluorescence intensities were quantified in the right section. (B) The polysome profiling of H1299 cells transiently transfected with the ALKBH4 plasmid or the pCDH vector was analyzed. (C) The nascent protein synthesis of H1299 cells transiently transfected with 5′-tsRNA^{Glu} mimics or NC mimics was determined using OPP protein synthesis assay. Their relative fluorescence intensities were quantified in the right section. (D) The polysome profiling of H1299 cells transiently transfected with 5′-tsRNA^{Glu} mimics or NC mimics was analyzed. Three independent experiments were performed in triplicate. Data are shown as the mean ± SD (two-sided independent Student's *t*-test, ** $p < 0.01$). Note: tsRNA-Glu is the abbreviation of 5′-tsRNA^{Glu}.

teins (Fig. 6C). Considering that RPL17 is a ribosomal large subunit protein closely associated with translation, we selected RPL17 for further validation. Independent RNA pull-down assays and WB assays confirmed the interaction of 5′-tsRNA^{Glu} and RPL17 in both H1299 and A549 cells (Fig. 6D). Consistently, RIP assays also proved that 5′-tsRNA^{Glu} was enriched by the RPL17 antibody group, compared with the IgG antibody group (Fig. 6E). In addition, 5′-tsRNA^{Glu} did not affect the expression of RPL17 (**Supplementary Fig. 6**). To gain insight into the specific binding pattern between 5′-tsRNA^{Glu} and RPL17, we utilized the online database HDOCK to predict the detailed binding sites of 5′-tsRNA^{Glu} to RPL17 (Fig. 6F). It showed that 5′-tsRNA^{Glu} bound to the region spanning residues 137-142 of RPL17, which corresponds to the protein-rRNA interaction interface. To determine the subcellular localization of 5′-tsRNA^{Glu}, we next performed nucleoplasmic separation assays and found that over 80% of 5′-tsRNA^{Glu} localized in the cytoplasm of both H1299 cells and A549 cells (Fig. 6G). Furthermore, we explored the distribution of 5′-tsRNA^{Glu} in the 40S, 60S, and 80S ribosomal fractions. The overexpression of 5′-tsRNA^{Glu} led to an increased ratio of 5′-tsRNA^{Glu} in the 60S but a decreased ratio of 5′-tsRNA^{Glu} in the 80S ribosomal fraction (Fig. 6H). Given these findings, we speculate that the binding of 5′-tsRNA^{Glu} to RPL17 disrupts the binding of RPL17 to rRNAs, and thus 80S ribosome assembly.

4. Discussion

ALKBH4 was initially characterized as a catalyst for actin demethylation that modulates the contraction of the actomyosin network [48–50]. Subsequent studies have revealed its potential role in regulating chromatin states and gene expression [51,52]. Although studies focused on the potential role of ALKBH4 in oncology are relatively scarce, current evidence suggests that it may function as a tumor

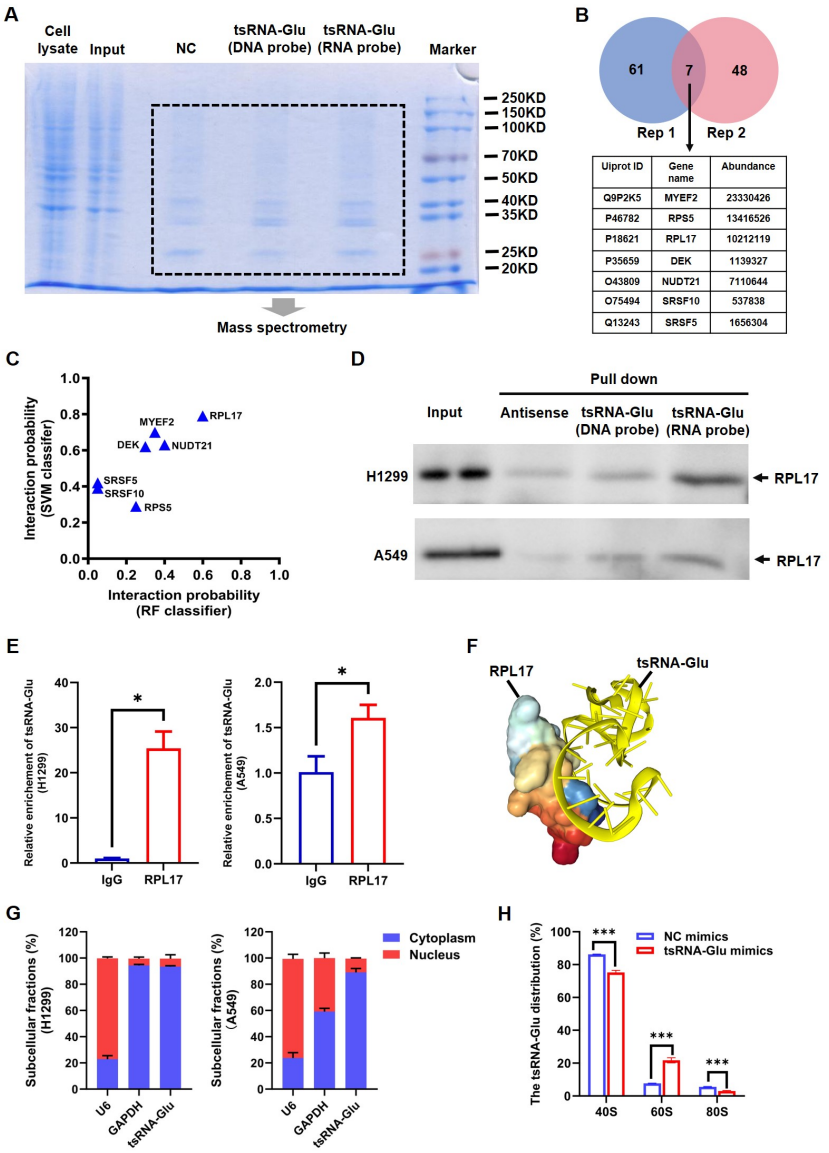

Fig. 6. 5′-tsRNA^{Glu} selectively interacts with RPL17. (A) SDS-PAGE and then Coomassie staining of RNA pull-down samples from H1299 cells. tsGlu (RNA Probe): 5′-tsRNA^{Glu}; tsGlu (DNA Probe): the corresponding DNA sequence of 5′-tsRNA^{Glu}; NC: the reverse complementary DNA sequence of 5′-tsRNA^{Glu}. (B) The counts of candidate 5′-tsRNA^{Glu} interacted proteins identified in two biological replicates as well as these seven overlapping proteins. (C) The interaction probability of 5′-tsRNA^{Glu} and candidate proteins predicted by RPIseq database. The horizontal axis represents the interaction probability using RF classifier, and the vertical axis represents the interaction probability using SVM classifier. (D) Validation of the binding of 5′-tsRNA^{Glu} to RPL17 using RNA pull-down assays. 5′-Biotinylated synthetic oligonucleotides were used for RNA pull-down assays. The antisense sequence of 5′-tsRNA^{Glu} was used as the negative control. Three independent experiments were performed in triplicate. (E) Validation of the binding of 5′-tsRNA^{Glu} to RPL17 using RIP assays. The 5′-tsRNA^{Glu} level in the product obtained from RIP was detected using quantitative RT-PCR. Three independent experiments were performed in triplicate. (F) The binding pattern of 5′-tsRNA^{Glu} and RPL17 protein predicted by HDOCK database. 5′-tsRNA^{Glu} is shown in yellow, which is predicted to bind to the protein-rRNA interface (spanning residues 137–142) of RPL17. (G) The levels of 5′-tsRNA^{Glu} in the cytoplasm and the nucleus of H1299 cells (left) and A549 cells (right) were determined using quantitative RT-PCR following subcellular RNA fractionation. GAPDH and U6 served as the controls for the cytoplasmic fraction and the nuclear fraction, respectively. Three independent experiments were performed in triplicate. Data are shown as the mean ± SD (two-sided independent Student's *t*-test. (H) Quantitative RT-PCR was utilized to detect the 5′-tsRNA^{Glu} level in 40S, 60S, and 80S ribosomal fractions obtained from H1299 cells transiently transfected with NC mimics or 5′-tsRNA^{Glu} mimics. Three independent experiments were performed in triplicate. Data are shown as the mean ± SD (two-sided independent Student's *t*-test, * $p < 0.05$, *** $p < 0.001$). Note: tsRNA-Glu is the abbreviation of 5′-tsRNA^{Glu}.

suppressor. In a previous study, Shen *et al*. [53] demonstrated that ALKBH4 suppressed the metastasis of colorectal cancer by inhibiting *miR-21* expression and epithelial-mesenchymal transition (EMT). This functionality was attributed to its competitive binding to the methyltransferase WDR5, which is responsible for H3K4me3 modification, leading to reduced H3K4me3 levels in the chromatin region associated with the WDR5 target gene *miR-21* [53]. Another study found that among the ALKBH family, only ALKBH4 was downregulated by hypoxia-inducible factor HIF-1α in head and neck, and breast cancer cell lines. The knockdown of ALKBH4 promoted EMT, cell migration, invasion, and growth *in vitro*, as well as tumor metastasis and growth *in vivo*. Conversely, the overexpression of ALKBH4 reserved these effects [54]. While those studies have predominantly characterized ALKBH4 as a tumor suppressor, the Tsujikawa group revealed its context-dependent function as a tumor promoter in NSCLC. They reported that ALKBH4 depletion suppressed E2F1 expression and its transcriptional targets, resulting in G1 phase arrest, diminished cell proliferation and tumorigenicity. The tumor-promoting activity of ALKBH4 was attributed to its demethylase activity, likely 6mA demethylation within DNA [55]. Further investigations by this group uncovered that ALKBH4 modulated uridine modification dynamics on tRNAs and thus translational efficiency [56]. Strikingly, our findings revealed an opposing function of ALKBH4 in NSCLC. In the present study, we observed that ALKBH4 significantly repressed the proliferative capacity of NSCLC cells and induced cell cycle arrest at the S phase (Fig. 3). Furthermore, ALKBH4 attenuated global translational efficiency by decreasing the levels of 40S, 60S, and 80S ribosomal subunits along with polysomes in NSCLC cells (Fig. 5). This suggests that ALKBH4 may exert dual functions depending on its subcellular localization, post-translational modifications, or interacting partners.

Our study further demonstrated that the inhibitory effect of ALKBH4 on the proliferation of NSCLC cells was dependent on 5′-tsRNA^{Glu}. Specifically, ALKBH4 induced the biogenesis of 5′-tsRNA^{Glu} in NSCLC cells (Fig. 2). 5′-tsRNA^{Glu} markedly suppressed the proliferation of NSCLC cells, arrested cell cycle arrest at the G2/M phase (Fig. 4), and attenuated global translational efficiency by decreasing the abundance of 80S ribosomes and polysomes (Fig. 5). Rescue assays further confirmed that ALKBH4 inhibited the proliferation of NSCLC cells via a 5′-tsRNA^{Glu}-mediated mechanism (Fig. 4F). It is plausible that the ALKBH4-induced production of 5′-tsRNA^{Glu} involves RNA modification. RNA molecules carry over 100 types of functional chemical modifications [35], whose dynamic and reversible regulation, along with their functional consequences, are coordinated by “writer”, “eraser” and “reader” proteins [36]. tRNAs harbor more chemical modifications than other RNA species, with an average of 13 modifications per molecule [57]; these modifications modulate tRNA stability and function through structural influences [58]. Methylation is the most abundant category of tRNA chemical modifications [59,60], including m^1A, m^1G, m^3C, m^5C, and $m^2{}_2G$ [61]. tRNA methyltransferases (“writers”) act in concert with tRNA demethylases (“erasers”) to dynamically regulate tRNA methylation. Reduced tRNA methylation can destabilize tRNAs, rendering them more susceptible to ribonuclease cleavage and leading to the biogenesis of tsRNA [36]. The ALKBH family comprises nine members (ALKBH1-ALKBH8 and FTO), many of which exhibit demethylase activity. For instance, Chen *et al*. [38] discovered that ALKBH3 catalyzed the demethylation of m^1A and m^3C in tRNAs. m^1A-demethylated tRNAs, in particular, were more prone to cleavage by ANG, predominantly yielding 5′-tsRNAs. ALKBH3 was shown to facilitate tumor cell proliferation, invasion, chemotherapy resistance, and tumorigenesis *in vivo* via specific tsRNAs such as 5′-tDR-GlyGCC [38]. Although ALKBH4 has not yet been definitely characterized as a tRNA demethylase, one study indicated that it could modulate translational efficiency through regulating uridine modifications in tRNAs [56]. To test the hypothesis that ALKBH4 catalyzes demethylation at specific sites of tRNA^{Glu}, thereby promoting its cleavage to generate 5′-tsRNA^{Glu}, future studies will employ liquid chromatography-tandem mass spectrometry (LC-MS/MS) to analyze the impact of ALKBH4 on nucleotide methylation levels at specific positions of tRNA^{Glu}.

Despite the growing interest in tsRNAs, the involvement of tsRNAs in lung cancer develpment remains poorly characterized. Early investigations revealed that tsRNA-46, tsRNA-47, and tsRNA-53 impaired the clonogenic potential of NSCLC cells via unknown mechanisms [23,32]. Subsequent work by Shao *et al*. [62] demonstrated that silencing a tiRNA derived from tRNALeu-CAG suppressed NSCLC cell proliferation and induced G0/G1 cell cycle arrest, putatively through downregulation of AURKA. Expanding on this, Young and colleagues uncovered that AS-tDR-007333 drove both proliferation and metastasis in NSCLC cells via the HSPB1-MED29 and ELK4-MED29 signaling axes [63]. In a distinct mechanistic paradigm, Yu *et al*. [33] identified CAT1, a pan-cancer-upregulated tsRNA, which stabilized NOTCH2 mRNA by binding RBPMS and subsequently abrogating CCR4-NOT-mediated deadenylation, thus facilitating lung cancer progression. More recently, Zhao *et al*. [64] found that tumor-derived exosomal 3′-tsRNA-AlaCGC activated the TGF-β/Smad3 pathway in fibroblasts, thereby inducing the synergistic action of SASP and Galactin-9 to confer immune tolerance in LUAD. In the present study, we identified 5′-tsRNA^{Glu} as a potent suppressor of NSCLC proliferation that induced G2/M phase arrest, an effect likely mediated through attenuating global translational efficiency. tsRNAs modulate translation through a variety of mechanisms, such as the miRNA-like suppression of target mRNAs [22,24,28,44,46,47], the repression of translation ini-

tiation via unique RG4 structures [10–13,21], the inhibition of translation initiation via specific tsRNA modifications [65], by binding to ribosomes to either impede or enhance translational activity [17,66], and by remodeling mRNA secondary structures to facilitate translational efficiency [18]. Our study revealed that 5′-tsRNA^{Glu} did not repress the translation of specific oncogenes through a miRNA-like mechanism (**Supplementary Fig. 5**). Instead, we confirmed that 5′-tsRNA^{Glu} bound directly to the large ribosomal subunit protein RPL17 (Fig. 6). Based on the observed enrichment of 5′-tsRNA^{Glu} in the 60S subunit and its decreased presence in the 80S monosome (Fig. 6H), together with structural modeling predicting its ability to bind to the RPL17-rRNA interface (Fig. 6F), we propose that the binding of 5′-tsRNA^{Glu} to RPL17 disrupts the interaction between RPL17 and rRNA, thereby hindering assembly of the 80S ribosome. Future studies will generate a series of truncated RPL17 mutants to identify the specific domain responsible for its interaction with 5′-tsRNA^{Glu}, and to further elucidate how the 5′-tsRNA^{Glu}-RPL17 interaction influences 80S ribosome assembly.

5. Limitations

While our study uncovers a previously unrecognized role of the ALKBH4/5′-tsRNA^{Glu} axis in modulating translational efficiency and cellular proliferation in NSCLC, several limitations warrant consideration. First, the precise molecular mechanism by which 5′-tsRNA^{Glu} binds to RPL17 to suppress translation and proliferation remains incompletely elucidated. Computational predications indicate that 5′-tsRNA^{Glu} interacts with a region spanning residues 137–142 of RPL17, corresponding to the protein-rRNA interaction interface, further studies employing systematic truncations of RPL17 are necessary to delineate the minimal binding domain and identify specific amino acid residues essential for 5′-tsRNA^{Glu} recognition. Furthermore, well-designed rescue experiments, wherein wild-type and mutant RPL17 constructs will be introduced to confirm whether the 5′-tsRNA^{Glu}-RPL17 interaction is directly responsible for the defects in 60S ribosomal subunit assembly, global translation efficiency, and proliferative capacity. Second, the diagnostic and therapeutic potential of the ALKBH4/5′-tsRNA^{Glu} axis has yet to be systematically evaluated. Future investigations should focus on collecting adequate cohorts of clinical peripheral blood specimens to assess the utility of ALKBH4 and 5′-tsRNA^{Glu} as non-invasive biomarkers for NSCLC diagnosis. In addition, *in vivo* xenograft models is imperative to determine whether targeting ALKBH4/5′-tsRNA^{Glu} represents a viable therapeutic target in NSCLC.

6. Conclusions

Our findings establish the ALKBH4/5′-tsRNA^{Glu} axis as a critical pathway suppressing the progression of NSCLC. ALKBH4 promotes the biogenesis of 5′-tsRNA^{Glu}, which in turn exerts tumor-suppressive effects that are unlike miRNA, but rather via direct interaction with the ribosomal protein RPL17. This interaction is proposed to destabilize the RPL17-rRNA interface, thereby impeding assembly of the 80S ribosome, thus attenuating global translational efficiency, and ultimately inhibiting cell proliferation. Therefore, this study implies both ALKBH4 and 5′-tsRNA^{Glu} represent promising candidates for the diagnosis and treatment of NSCLC.

Abbreviations

tsRNAs, tRNA-derived small RNAs; ALKBH, alpha-ketoglutarate-dependent dioxygenase alkB homolog; NSCLC, non-small cell lung cancer; LUAD, lung adenocarcinoma; LSCC, lung squamous cell carcinoma; ncRNAs, non-coding RNAs; UV, ultraviolet; ANG, angiogenin; tiRNAs, tRNA-derived stress-induced RNAs; RG4, RNA G-quadruplexes; ASO, antisense oligonucleotide; PI, propidium iodide; CHX, cycloheximide; LC-MS/MS, liquid chromatography-tandem mass spectrometry; RIP, RNA immunoprecipitation; FDR, false discovery rate.

Availability of Data and Materials

The datasets used and analyzed during the current study are available from the corresponding author on reasonable request.

Author Contributions

CS: Investigation, Methodology, Writing – original draft. HC: Investigation, Methodology, Writing – original draft. YL: Investigation, Methodology. DX: Investigation, Methodology. WD: Data curation, Software, Validation. MP: Data curation, Software, Validation. LS: Data curation, Software, Validation. JT: Validation. YZ: Conceptualization, Funding acquisition, Project administration, Writing – review and editing. All authors contributed to editorial changes in the manuscript. All authors read and approved the final manuscript. All authors have participated sufficiently in the work and agreed to be accountable for all aspects of the work.

Ethics Approval and Consent to Participate

Not applicable.

Acknowledgment

Not applicable.

Funding

This research was funded by Chongqing Natural Science Foundation (CSTB2022NSCQ-MSX0123).

Conflict of Interest

The authors declare no conflict of interest.

Supplementary Material

Supplementary material associated with this article can be found, in the online version, at https://doi.org/10.31083/FBL50109.

References

[1] Han B, Zheng R, Zeng H, Wang S, Sun K, Chen R, *et al*. Cancer incidence and mortality in China, 2022. Journal of the National Cancer Center. 2024; 4: 47–53. https://doi.org/10.1016/j.jncc.2024.01.006.

[2] Chen Z, Fillmore CM, Hammerman PS, Kim CF, Wong KK. Non-small-cell lung cancers: a heterogeneous set of diseases. Nature Reviews. Cancer. 2014; 14: 535–546. https://doi.org/10.1038/nrc3775.

[3] Xu D, Qiao D, Lei Y, Zhang C, Bu Y, Zhang Y. Transfer RNA-derived small RNAs (tsRNAs): Versatile regulators in cancer. Cancer Letters. 2022; 546: 215842. https://doi.org/10.1016/j.canlet.2022.215842.

[4] Chen Q, Zhou T. Emerging functional principles of tRNA-derived small RNAs and other regulatory small RNAs. The Journal of Biological Chemistry. 2023; 299: 105225. https://doi.org/10.1016/j.jbc.2023.105225.

[5] Shi J, Zhou T, Chen Q. Exploring the expanding universe of small RNAs. Nature Cell Biology. 2022; 24: 415–423. https://doi.org/10.1038/s41556-022-00880-5.

[6] Chen Q, Zhang X, Shi J, Yan M, Zhou T. Origins and evolving functionalities of tRNA-derived small RNAs. Trends in Biochemical Sciences. 2021; 46: 790–804. https://doi.org/10.1016/j.tibs.2021.05.001.

[7] Kuhle B, Chen Q, Schimmel P. tRNA renovatio: Rebirth through fragmentation. Molecular Cell. 2023; 83: 3953–3971. https://doi.org/10.1016/j.molcel.2023.09.016.

[8] Yamasaki S, Ivanov P, Hu GF, Anderson P. Angiogenin cleaves tRNA and promotes stress-induced translational repression. The Journal of Cell Biology. 2009; 185: 35–42. https://doi.org/10.1083/jcb.200811106.

[9] Emara MM, Ivanov P, Hickman T, Dawra N, Tisdale S, Kedersha N, *et al*. Angiogenin-induced tRNA-derived stress-induced RNAs promote stress-induced stress granule assembly. The Journal of Biological Chemistry. 2010; 285: 10959–10968. https://doi.org/10.1074/jbc.M109.077560.

[10] Ivanov P, O'Day E, Emara MM, Wagner G, Lieberman J, Anderson P. G-quadruplex structures contribute to the neuroprotective effects of angiogenin-induced tRNA fragments. Proceedings of the National Academy of Sciences of the United States of America. 2014; 111: 18201–18206. https://doi.org/10.1073/pnas.1407361111.

[11] Lyons SM, Achorn C, Kedersha NL, Anderson PJ, Ivanov P. YB-1 regulates tiRNA-induced Stress Granule formation but not translational repression. Nucleic Acids Research. 2016; 44: 6949–6960. https://doi.org/10.1093/nar/gkw418.

[12] Lyons SM, Gudanis D, Coyne SM, Gdaniec Z, Ivanov P. Identification of functional tetramolecular RNA G-quadruplexes derived from transfer RNAs. Nature Communications. 2017; 8: 1127. https://doi.org/10.1038/s41467-017-01278-w.

[13] Lyons SM, Kharel P, Akiyama Y, Ojha S, Dave D, Tsvetkov V, *et al*. eIF4G has intrinsic G-quadruplex binding activity that is required for tiRNA function. Nucleic Acids Research. 2020; 48: 6223–6233. https://doi.org/10.1093/nar/gkaa336.

[14] Guzzi N, Cieśla M, Ngoc PCT, Lang S, Arora S, Dimitriou M, *et al*. Pseudouridylation of tRNA-Derived Fragments Steers Translational Control in Stem Cells. Cell. 2018; 173: 1204–1216.e26. https://doi.org/10.1016/j.cell.2018.03.008.

[15] Guzzi N, Muthukumar S, Cieśla M, Todisco G, Ngoc PCT, Madej M, *et al*. Pseudouridine-modified tRNA fragments repress aberrant protein synthesis and predict leukaemic progression in myelodysplastic syndrome. Nature Cell Biology. 2022; 24: 299–306. https://doi.org/10.1038/s41556-022-00852-9.

[16] Luo S, He F, Luo J, Dou S, Wang Y, Guo A, *et al*. Drosophila tsRNAs preferentially suppress general translation machinery via antisense pairing and participate in cellular starvation response. Nucleic Acids Research. 2018; 46: 5250–5268. https://doi.org/10.1093/nar/gky189.

[17] Fricker R, Brogli R, Luidalepp H, Wyss L, Fasnacht M, Joss O, *et al*. A tRNA half modulates translation as stress response in Trypanosoma brucei. Nature Communications. 2019; 10: 118. https://doi.org/10.1038/s41467-018-07949-6.

[18] Kim HK, Fuchs G, Wang S, Wei W, Zhang Y, Park H, *et al*. A transfer-RNA-derived small RNA regulates ribosome biogenesis. Nature. 2017; 552: 57–62. https://doi.org/10.1038/nature25005.

[19] Haussecker D, Huang Y, Lau A, Parameswaran P, Fire AZ, Kay MA. Human tRNA-derived small RNAs in the global regulation of RNA silencing. RNA (New York, N.Y.). 2010; 16: 673–695. https://doi.org/10.1261/rna.2000810.

[20] Zhang Y, Shi J, Rassoulzadegan M, Tuorto F, Chen Q. Sperm RNA code programmes the metabolic health of offspring. Nature Reviews. Endocrinology. 2019; 15: 489–498. https://doi.org/10.1038/s41574-019-0226-2.

[21] Ivanov P, Emara MM, Villen J, Gygi SP, Anderson P. Angiogenin-induced tRNA fragments inhibit translation initiation. Molecular Cell. 2011; 43: 613–623. https://doi.org/10.1016/j.molcel.2011.06.022.

[22] Balatti V, Rizzotto L, Miller C, Palamarchuk A, Fadda P, Pandolfo R, *et al*. TCL1 targeting miR-3676 is codeleted with tumor protein p53 in chronic lymphocytic leukemia. Proceedings of the National Academy of Sciences of the United States of America. 2015; 112: 2169–2174. https://doi.org/10.1073/pnas.1500010112.

[23] Pekarsky Y, Balatti V, Palamarchuk A, Rizzotto L, Veneziano D, Nigita G, *et al*. Dysregulation of a family of short noncoding RNAs, tsRNAs, in human cancer. Proceedings of the National Academy of Sciences of the United States of America. 2016; 113: 5071–5076. https://doi.org/10.1073/pnas.1604266113.

[24] Maute RL, Schneider C, Sumazin P, Holmes A, Califano A, Basso K, *et al*. tRNA-derived microRNA modulates proliferation and the DNA damage response and is down-regulated in B cell lymphoma. Proceedings of the National Academy of Sciences of the United States of America. 2013; 110: 1404–1409. https://doi.org/10.1073/pnas.1206761110.

[25] Goodarzi H, Liu X, Nguyen HCB, Zhang S, Fish L, Tavazoie SF. Endogenous tRNA-Derived Fragments Suppress Breast Cancer Progression via YBX1 Displacement. Cell. 2015; 161: 790–802. https://doi.org/10.1016/j.cell.2015.02.053.

[26] Liu X, Mei W, Padmanaban V, Alwaseem H, Molina H, Passarelli MC, *et al*. A pro-metastatic tRNA fragment drives Nucleolin oligomerization and stabilization of its bound metabolic mRNAs. Molecular Cell. 2022; 82: 2604–2617.e8. https://doi.org/10.1016/j.molcel.2022.05.008.

[27] Honda S, Loher P, Shigematsu M, Palazzo JP, Suzuki R, Imoto I, *et al*. Sex hormone-dependent tRNA halves enhance cell proliferation in breast and prostate cancers. Proceedings of the National Academy of Sciences of the United States of America. 2015; 112: E3816–E3825. https://doi.org/10.1073/pnas.1510077112.

[28] Huang B, Yang H, Cheng X, Wang D, Fu S, Shen W, *et al*. tRF/miR-1280 Suppresses Stem Cell-like Cells and Metastasis in Colorectal Cancer. Cancer Research. 2017; 77: 3194–3206. https://doi.org/10.1158/0008-5472.CAN-16-3146.

[29] Li S, Shi X, Chen M, Xu N, Sun D, Bai R, *et al*. Angiogenin promotes colorectal cancer metastasis via tiRNA produc-

tion. International Journal of Cancer. 2019; 145: 1395–1407. https://doi.org/10.1002/ijc.32245.
[30] Cui H, Li H, Wu H, Du F, Xie X, Zeng S, *et al*. A novel 3'tRNA-derived fragment tRF-Val promotes proliferation and inhibits apoptosis by targeting EEF1A1 in gastric cancer. Cell Death & Disease. 2022; 13: 471. https://doi.org/10.1038/s41419-022-04930-6.
[31] Xiong Q, Zhang Y, Xu Y, Yang Y, Zhang Z, Zhou Y, *et al*. tiRNA-Val-CAC-2 interacts with FUBP1 to promote pancreatic cancer metastasis by activating c MYC transcription. Oncogene. 2024; 43: 1274–1287. https://doi.org/10.1038/s41388-024-02991-9.
[32] Balatti V, Nigita G, Veneziano D, Drusco A, Stein GS, Messier TL, *et al*. tsRNA signatures in cancer. Proceedings of the National Academy of Sciences of the United States of America. 2017; 114: 8071–8076. https://doi.org/10.1073/pnas.1706908114.
[33] Yu M, Yi J, Qiu Q, Yao D, Li J, Yang J, *et al*. Pan-cancer tRNA-derived fragment CAT1 coordinates RBPMS to stabilize NOTCH2 mRNA to promote tumorigenesis. Cell Reports. 2023; 42: 113408. https://doi.org/10.1016/j.celrep.2023.113408.
[34] Shi J, Zhang Y, Tan D, Zhang X, Yan M, Zhang Y, *et al*. PANDORA-seq expands the repertoire of regulatory small RNAs by overcoming RNA modifications. Nature Cell Biology. 2021; 23: 424–436. https://doi.org/10.1038/s41556-021-00652-7.
[35] Frye M, Jaffrey SR, Pan T, Rechavi G, Suzuki T. RNA modifications: what have we learned and where are we headed? Nature Reviews. Genetics. 2016; 17: 365–372. https://doi.org/10.1038/nrg.2016.47.
[36] Zhang X, Cozen AE, Liu Y, Chen Q, Lowe TM. Small RNA Modifications: Integral to Function and Disease. Trends in Molecular Medicine. 2016; 22: 1025–1034. https://doi.org/10.1016/j.molmed.2016.10.009.
[37] Rashad S, Han X, Sato K, Mishima E, Abe T, Tominaga T, *et al*. The stress specific impact of ALKBH1 on tRNA cleavage and tiRNA generation. RNA Biology. 2020; 17: 1092–1103. https://doi.org/10.1080/15476286.2020.1779492.
[38] Chen Z, Qi M, Shen B, Luo G, Wu Y, Li J, *et al*. Transfer RNA demethylase ALKBH3 promotes cancer progression via induction of tRNA-derived small RNAs. Nucleic Acids Research. 2019; 47: 2533–2545. https://doi.org/10.1093/nar/gky1250.
[39] A Alemu E, He C, Klungland A. ALKBHs-facilitated RNA modifications and de-modifications. DNA Repair. 2016; 44: 87–91. https://doi.org/10.1016/j.dnarep.2016.05.026.
[40] Ji Y, Xie M, Lan H, Zhang Y, Long Y, Weng H, *et al*. PRR11 is a novel gene implicated in cell cycle progression and lung cancer. The International Journal of Biochemistry & Cell Biology. 2013; 45: 645–656. https://doi.org/10.1016/j.biocel.2012.12.002.
[41] Cancer Genome Atlas Research Network. Comprehensive genomic characterization of squamous cell lung cancers. Nature. 2012; 489: 519–525. https://doi.org/10.1038/nature11404.
[42] Yu G, Wang LG, Han Y, He QY. clusterProfiler: an R package for comparing biological themes among gene clusters. Omics: a Journal of Integrative Biology. 2012; 16: 284–287. https://doi.org/10.1089/omi.2011.0118.
[43] Holste D, Huo G, Tung V, Burge CB. HOLLYWOOD: a comparative relational database of alternative splicing. Nucleic Acids Research. 2006; 34: D56–D62. https://doi.org/10.1093/nar/gkj048.
[44] Zhou K, Diebel KW, Holy J, Skildum A, Odean E, Hicks DA, *et al*. A tRNA fragment, tRF5-Glu, regulates BCAR3 expression and proliferation in ovarian cancer cells. Oncotarget. 2017; 8: 95377–95391. https://doi.org/10.18632/oncotarget.20709.
[45] Tong L, Zhang W, Qu B, Zhang F, Wu Z, Shi J, *et al*. The tRNA-Derived Fragment-3017A Promotes Metastasis by Inhibiting NELL2 in Human Gastric Cancer. Frontiers in Oncology. 2021; 10: 570916. https://doi.org/10.3389/fonc.2020.570916.
[46] Mo D, Jiang P, Yang Y, Mao X, Tan X, Tang X, *et al*. A tRNA fragment, 5'-tiRNA^{Val}, suppresses the Wnt/β-catenin signaling pathway by targeting FZD3 in breast cancer. Cancer Letters. 2019; 457: 60–73. https://doi.org/10.1016/j.canlet.2019.05.007.
[47] Mo D, He F, Zheng J, Chen H, Tang L, Yan F. tRNA-Derived Fragment tRF-17-79MP9PP Attenuates Cell Invasion and Migration *via* THBS1/TGF-β1/Smad3 Axis in Breast Cancer. Frontiers in Oncology. 2021; 11: 656078. https://doi.org/10.3389/fonc.2021.656078.
[48] Li MM, Nilsen A, Shi Y, Fusser M, Ding YH, Fu Y, *et al*. ALKBH4-dependent demethylation of actin regulates actomyosin dynamics. Nature Communications. 2013; 4: 1832. https://doi.org/10.1038/ncomms2863.
[49] Sun Q, Liu X, Gong B, Wu D, Meng A, Jia S. Alkbh4 and Atrn Act Maternally to Regulate Zebrafish Epiboly. International Journal of Biological Sciences. 2017; 13: 1051–1066. https://doi.org/10.7150/ijbs.19203.
[50] Nilsen A, Fusser M, Greggains G, Fedorcsak P, Klungland A. ALKBH4 depletion in mice leads to spermatogenic defects. PloS One. 2014; 9: e105113. https://doi.org/10.1371/journal.pone.0105113.
[51] Bjørnstad LG, Meza TJ, Otterlei M, Olafsrud SM, Meza-Zepeda LA, Falnes PØ. Human ALKBH4 interacts with proteins associated with transcription. PloS One. 2012; 7: e49045. https://doi.org/10.1371/journal.pone.0049045.
[52] Kweon SM, Chen Y, Moon E, Kvederaviciutė K, Klimasauskas S, Feldman DE. An Adversarial DNA N^6-Methyladenine-Sensor Network Preserves Polycomb Silencing. Molecular Cell. 2019; 74: 1138–1147.e6. https://doi.org/10.1016/j.molcel.2019.03.018.
[53] Shen C, Yan T, Tong T, Shi D, Ren L, Zhang Y, *et al*. ALKBH4 Functions as a Suppressor of Colorectal Cancer Metastasis via Competitively Binding to WDR5. Frontiers in Cell and Developmental Biology. 2020; 8: 293. https://doi.org/10.3389/fcell.2020.00293.
[54] Chen JL, Peng PH, Wu HT, Chen DR, Hsieh CY, Chang JS, *et al*. ALKBH4 functions as a hypoxia-responsive tumor suppressor and inhibits metastasis and tumorigenesis. Cellular Oncology (Dordrecht, Netherlands). 2025; 48: 425–435. https://doi.org/10.1007/s13402-024-01004-x.
[55] Jingushi K, Aoki M, Ueda K, Kogaki T, Tanimoto M, Monoe Y, *et al*. ALKBH4 promotes tumourigenesis with a poor prognosis in non-small-cell lung cancer. Scientific Reports. 2021; 11: 8677. https://doi.org/10.1038/s41598-021-87763-1.
[56] Kogaki T, Hase H, Tanimoto M, Tashiro A, Kitae K, Ueda Y, *et al*. ALKBH4 is a novel enzyme that promotes translation through modified uridine regulation. The Journal of Biological Chemistry. 2023; 299: 105093. https://doi.org/10.1016/j.jbc.2023.105093.
[57] Saikia M, Fu Y, Pavon-Eternod M, He C, Pan T. Genome-wide analysis of N1-methyl-adenosine modification in human tRNAs. RNA (New York, N.Y.). 2010; 16: 1317–1327. https://doi.org/10.1261/rna.2057810.
[58] Novoa EM, Pavon-Eternod M, Pan T, Ribas de Pouplana L. A role for tRNA modifications in genome structure and codon usage. Cell. 2012; 149: 202–213. https://doi.org/10.1016/j.cell.2012.01.050.
[59] Oerum S, Dégut C, Barraud P, Tisné C. m1A Post-Transcriptional Modification in tRNAs. Biomolecules. 2017; 7: 20. https://doi.org/10.3390/biom7010020.
[60] Roundtree IA, Evans ME, Pan T, He C. Dynamic RNA Modifications in Gene Expression Regulation. Cell. 2017; 169: 1187–1200. https://doi.org/10.1016/j.cell.2017.05.045.
[61] Phizicky EM, Hopper AK. tRNA biology charges to the front. Genes & Development. 2010; 24: 1832–1860. https://doi.org/

10.1101/gad.1956510.
[62] Shao Y, Sun Q, Liu X, Wang P, Wu R, Ma Z. tRF-Leu-CAG promotes cell proliferation and cell cycle in non-small cell lung cancer. Chemical Biology & Drug Design. 2017; 90: 730–738. https://doi.org/10.1111/cbdd.12994.
[63] Yang W, Gao K, Qian Y, Huang Y, Xiang Q, Chen C, *et al*. A novel tRNA-derived fragment AS-tDR-007333 promotes the malignancy of NSCLC via the HSPB1/MED29 and ELK4/MED29 axes. Journal of Hematology & Oncology. 2022; 15: 53. https://doi.org/10.1186/s13045-022-01270-y.
[64] Zhao G, Zhang Y, Zhang H, Guo Y, Xu C, Ge D, *et al*. Tumor-derived exosomal tsRNA 3'tiRNA-AlaCGC in promoting fibroblast senescence and Galectin-9 secretion to induce immune tolerance in lung adenocarcinoma. Cell Death Discovery. 2025; 11: 403. https://doi.org/10.1038/s41420-025-02695-3.
[65] Zuo Y, Zhu L, Guo Z, Liu W, Zhang J, Zeng Z, *et al*. tsRBase: a comprehensive database for expression and function of tsRNAs in multiple species. Nucleic Acids Research. 2021; 49: D1038–D1045. https://doi.org/10.1093/nar/gkaa888.
[66] Gebetsberger J, Zywicki M, Künzi A, Polacek N. tRNA-derived fragments target the ribosome and function as regulatory non-coding RNA in Haloferax volcanii. Archaea (Vancouver, B.C.). 2012; 2012: 260909. https://doi.org/10.1155/2012/260909.